

Coulomb interactions in charged fluids

Graziano Vernizzi,^{1,*} Guillermo Iván Guerrero-García,² and Monica Olvera de la Cruz^{2,3,4}

¹*Department of Physics and Astronomy, Siena College, Loudonville, New York 12211, USA*

²*Department of Materials Science, Northwestern University, Evanston, Illinois 60208, USA*

³*Department of Chemical Engineering, Northwestern University, Evanston, Illinois 60208, USA*

⁴*Department of Chemistry, Northwestern University, Evanston, Illinois 60208, USA*

(Received 10 August 2010; revised manuscript received 22 May 2011; published 25 July 2011)

The use of Ewald summation schemes for calculating long-range Coulomb interactions, originally applied to ionic crystalline solids, is a very common practice in molecular simulations of charged fluids at present. Such a choice imposes an artificial periodicity which is generally absent in the liquid state. In this paper we propose a simple analytical $O(N^2)$ method which is based on Gauss's law for computing exactly the Coulomb interaction between charged particles in a simulation box, when it is averaged over all possible orientations of a surrounding infinite lattice. This method mitigates the periodicity typical of crystalline systems and it is suitable for numerical studies of ionic liquids, charged molecular fluids, and colloidal systems with Monte Carlo and molecular dynamics simulations.

DOI: [10.1103/PhysRevE.84.016707](https://doi.org/10.1103/PhysRevE.84.016707)

PACS number(s): 05.10.-a, 82.70.Dd, 41.20.Cv, 61.20.Gy

I. INTRODUCTION

A challenging problem that still plagues modern numerical simulations is how to include long-range electrostatic interactions in a tractable way, a question that in its most general formulation lies undefeated [1]. In infinite periodic crystalline systems this problem has been overcome in the last century by using an approach originally proposed by Ewald [2], which allows the calculation of electrostatic energies per unit cell and of the respective Madelung constants [3,4]. This motivated the use of such methodology in ionic liquids, and nowadays Ewald-like schemes are frequently used to take into account long-range interactions not only in charged liquids, but also in the modeling of complex biological molecules in solution that interact electrostatically [5]. The importance of such Coulomb systems has prompted the improvement of the original performance of $O(N^2)$ operations, advancing to $O(N \log N)$ in [6], or even to $O(N)$ [7,8], with sophisticated computational schemes (for an extensive list, see [9]). Despite their significant success, it must be noted that Ewald-like schemes impose an artificial ordering typical of crystalline systems, which is not expected in the liquid state. Thus a desirable advance in the simulation of charged liquids would be the ability of computing electrostatic long-range interactions correctly, while including the natural isotropy and homogeneity of fluids at the same time. This is the main issue we address in the present work.

II. THEORETICAL APPROACH

In numerical simulations, the root of the problem stated in the Introduction is that forcing long-range electrostatics inside a *computational box* leaves the splintery question of what to do with the interactions at the box boundaries, where the long-range nature of electrostatics does not end obviously. One of the most popular choices, even in simulations of fluids, is to adopt periodic boundary conditions. Simply stated, it

means that a system of N charges q_i ($i = 1, \dots, N$) each at position \mathbf{b}_i is endowed with an infinite set of identical copies (*images*) that stem from identifying the simulation box as the primitive cell of an infinite regular lattice. In mathematical terms, let \mathbf{a}_1 , \mathbf{a}_2 , and \mathbf{a}_3 be three vectors that define the three-dimensional primitive cell, then any other cell of the periodic lattice is identified by the lattice vector $\mathbf{\Lambda} = n_1\mathbf{a}_1 + n_2\mathbf{a}_2 + n_3\mathbf{a}_3$, $n_i \in \mathbb{Z}$. The set $\{\mathbf{r}_i\}$ of the positions of all charges is $\mathbf{r}_i = \mathbf{b}_i + \mathbf{\Lambda}$, $\forall \mathbf{\Lambda}$, $i = 1, 2, \dots, N$. The total electrostatic energy of such a periodic system is infinite. It is therefore meaningful to consider the electrostatic energy *per* unit cell:

$$U = \frac{1}{2} \sum'_{\mathbf{\Lambda}, i, j} \frac{q_i q_j}{|\mathbf{r}_i - \mathbf{r}_j|}, \quad \mathbf{r}_i = \mathbf{b}_i, \mathbf{r}_j = \mathbf{b}_j + \mathbf{\Lambda}, \quad (1)$$

where the N charges interact purely via Coulomb forces within an homogeneous isotropic dielectric environment. The sum over i is for the charges in the main cell ($\mathbf{\Lambda} = \mathbf{0}$, $\mathbf{r}_i = \mathbf{b}_i$) while the sum over j and $\mathbf{\Lambda}$ is for all charges in the lattice. The prime symbol indicates that pairs such that $|\mathbf{r}_i - \mathbf{r}_j| = 0$ are excluded from the sum.

As we mentioned earlier, Eq. (1) is exact for systems with long-range order, such as ionic crystalline solids. However, for ionic fluids it is just an approximation [5]. The advantage of imposing an artificial periodicity is that Eq. (1) is tractable analytically (besides legitimate questions about its mathematical meaning, being a conditionally convergent sum [10]). A most praised equivalent formula was introduced by Ewald [2], who recast the summation into a form where the charges interact with each other via an effective interaction that includes all the periodic image contributions. Namely, long-range terms are expressed in the reciprocal lattice \mathbf{Q} (defined by $\mathbf{Q} \cdot \mathbf{\Lambda} = 2\pi m$, $m \in \mathbb{Z}$), and the total energy reads

$$U = U_Q + U_\Lambda + U_0 + U_d, \quad (2)$$

where the Fourier part is $U_Q = 2\pi \sum_{\mathbf{Q} \neq \mathbf{0}} \hat{q}(\mathbf{Q}) \hat{q}(-\mathbf{Q}) \exp(-Q^2/4\alpha^2)/VQ^2$, the real space part is $U_\Lambda = \sum'_{\mathbf{\Lambda}, i, j} q_i q_j \text{erfc}(D\alpha)/2D$, the constant contribution is $U_0 = -\alpha \sum_i q_i^2/\sqrt{\pi}$, and the dipolar contribution is

*gvernizzi@siena.edu

$U_d = 2\pi(\sum_i q_i \mathbf{b}_i)^2/3V$ [11]. The cell volume is $V = \mathbf{a}_1 \cdot (\mathbf{a}_2 \times \mathbf{a}_3)$, $D = |\mathbf{b}_i - \mathbf{b}_j - \mathbf{\Lambda}|$, and α is a parameter that in practical applications can be fixed by requiring $\partial U/\partial \alpha = 0$ [12] (if the \sum_Q and \sum_Λ are not truncated, then U is always independent from α). A derivation of Eq. (2) is presented in the Appendix. A crucial requirement for the validity of Eq. (2) is that the system must be globally electroneutral. In the rest of this paper we too assume $\sum_i q_i = 0$.

In order to tame the unwanted artifacts in simulations of ionic fluids due to the existence of preferential crystalline directions and planes of symmetry, a number of authors suggested performing a spherical average of U over all possible orientations of the lattice, or considered analogous isotropic radial potentials [13–15]. Such a strategy leads to new effective potentials between charges, and it has been generalized to other types of interactions such as dipolar, multipolar, power law, Lennard-Jones, and exponential potentials [15]. Numerical studies that explored the validity of such computational schemes seem to endorse the effectiveness of such an approximation (see, e.g., [16,17]; the list is not exhaustive). Despite the optimistic outlook, the recipe of taking a spherical average of a periodic structure might seem certainly a circuitous approach at first, since a heterogeneous system cannot be both infinitely periodic and spherically symmetric at the same time. This relates to the common assumption of previous approaches, that the simulation box is itself somewhat homogeneous.

The main focus of this paper is to (re)analyze such a problem from a slightly more fundamental standpoint based on the application of Gauss's law. We obtain a new formula for the spherically averaged periodic potential as we show below. We begin by assuming that since a liquid is characterized by a finite correlation length among its constituents, all long-range ordering is inconspicuous. Therefore if one imposes a periodicity on the primitive cell (which is larger than the fluid correlation length), the actual position of the periodic images should be of little relevance in the computation of physical quantities, and consequently they should have little or no influence on the structure, dynamics, and thermodynamics of the charges within the simulation box. Ergo the orientation of the lattice must be irrelevant for a liquid system with a typical correlation length smaller than the simulation box size, and different, rotated lattices should lead to the same physics (see Fig. 1). For the sake of preciseness, we define a *rotated lattice* by

$$\mathbf{\Lambda}(O) = O\mathbf{\Lambda} = \sum_{i=1}^3 n_i \mathbf{a}_i(O), \quad \mathbf{a}_i(O) = O\mathbf{a}_i, \quad (3)$$

where O is a 3×3 rotation matrix. The new positions are $\mathbf{r}_i(O) = \mathbf{b}_i + \mathbf{\Lambda}(O)$, meaning that all charges in the main cell are unaffected by the rotation and only the periodic images are actually rotated (see Fig. 1). Let $U(O)$ from Eq. (1) be the electrostatic energy of the rotated lattice. We then define the spherical average over all possible orientations of the lattice as

$$\langle U \rangle = \frac{1}{8\pi^2} \int_{SO(3)} dO U(O). \quad (4)$$

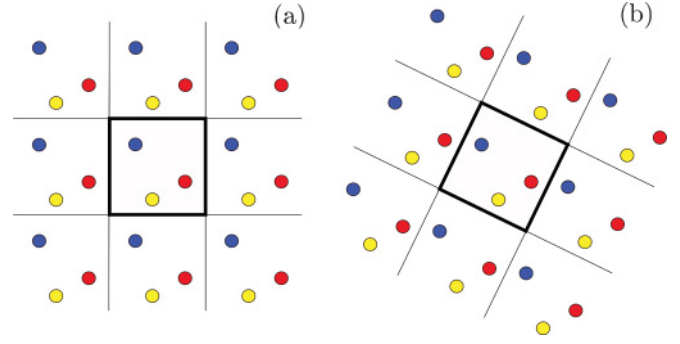


FIG. 1. (Color online) The positions of the periodic images of the main cell (square with thick borders) depend on the orientation of the lattice. The arrangement of charges in the rotated periodic lattice (b) differs from the one in the original lattice (a). Only the charges in the main cell are *not* affected by the rotation of the lattice.

The average is over all orthogonal 3×3 matrices representing proper rotations ($\det O = 1$), that is, the group $SO(3)$. The volume of the group $SO(3)$ is $8\pi^2$. We remind that since each rotation matrix can be parametrized by three parameters, the integral in Eq. (4) is a three-dimensional integral. By substituting Eq. (1) into Eq. (4), and under the assumption that the integral and the summation commute, we obtain

$$\langle U \rangle = \frac{1}{2} \sum'_{\Lambda, i, j} q_i \int_0^\pi d\omega 2(1 - \cos \omega) \times \int d\Omega \frac{q_j}{8\pi^2} \frac{1}{|\mathbf{b}_i - \mathbf{b}_j - O(\omega, \Omega)\mathbf{\Lambda}|}, \quad (5)$$

where we introduced the convenient axis-angle representation of a generic $SO(3)$ matrix, i.e., the angle ω around the rotation axis $\hat{\mathbf{n}} \in \Omega$, Ω being the unit sphere. The factor $2(1 - \cos \omega)$ is the density of rotation matrices in the axis-angle parameter space. The key remark now is that each Ω integral in the summation can be interpreted as the potential at \mathbf{b}_i generated by a spherical charge distribution centered at \mathbf{b}_j , with radius $|O\mathbf{\Lambda}| = |\mathbf{\Lambda}|$ and with charge density $q_j/(4\pi|\mathbf{\Lambda}|^2)$ [18]. Such a simple observation allows us to evaluate all integrals exactly. In fact, according to Gauss's law the electrostatic potential V generated by a density of charges distributed uniformly over a sphere of radius R , with charge density σ (hence with total charge $Q = 4\pi R^2\sigma$), and vanishing at infinity is $V(r) = Q/R$ for $r \leq R$ and $V(r) = Q/r$ for $r > R$, where r is the distance from the center of the sphere. We use the compact notation $V(r) = \frac{Q}{R} + (\frac{Q}{r} - \frac{Q}{R})\theta(r - R)$ where $\theta(x)$ is the unit step function: $\theta(x) = 0$ for $x \leq 0$ and $\theta(x) = 1$ for $x > 0$. In the degenerate case with $R = 0$ the potential is simply $V(r) = Q/r$. We thus obtain

$$\langle U \rangle = \frac{1}{2} \sum'_{i, j} \frac{q_i q_j}{|\mathbf{b}_i - \mathbf{b}_j|} + \frac{1}{2} \sum_{\Lambda \neq 0, i, j} q_i q_j \left[\frac{1}{|\mathbf{\Lambda}|} + \left(\frac{1}{|\mathbf{b}_i - \mathbf{b}_j|} - \frac{1}{|\mathbf{\Lambda}|} \right) \theta(|\mathbf{b}_i - \mathbf{b}_j| - |\mathbf{\Lambda}|) \right], \quad (6)$$

where we isolated the contribution from $\mathbf{\Lambda} = \mathbf{0}$. The first term in the second summation symbol is identically zero because of the electroneutrality condition $\sum_i q_i = 0$. Moreover, the distance $|\mathbf{b}_i - \mathbf{b}_j|$ cannot be larger than

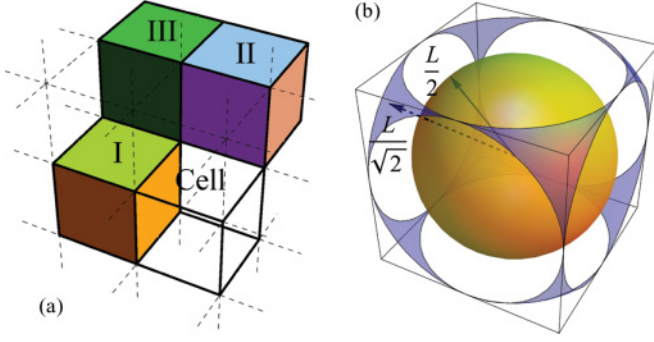


FIG. 2. (Color online) (a) Three different kinds of nearest neighbors of a cubic cell. (b) Regions of the main cell where the corrections to the Coulomb potential are relevant.

the size of the main cell, which in the conventional case of a cubic simulation box of size L is $|\mathbf{b}_i - \mathbf{b}_j| \leq \sqrt{3}L$. In this case we also have $|\mathbf{A}| = L\sqrt{n_1^2 + n_2^2 + n_3^2} = 0, L, \sqrt{2}L, \sqrt{3}L, \sqrt{4}L, \sqrt{5}L, \sqrt{6}L, \sqrt{8}L, \dots$. However, only two terms survive the limits imposed by the θ function, that is, when $|\mathbf{A}| = L$ and $|\mathbf{A}| = \sqrt{2}L$.

They correspond to two shells of periodic cells surrounding the simulation box (see Fig. 2), and they are precisely the 6 first nearest neighbors with a face in common with the main cell (type I), and the 12 nearest neighbors with an edge in common (type II). We note explicitly that the 8 nearest neighbors with a corner in common with the main cell (type III) do not contribute to the average energy. The final form of Eq. (6), which is also our main result, therefore reads

$$\begin{aligned} \langle U \rangle = & \frac{1}{2} \sum'_{i,j} \left\{ \frac{q_i q_j}{|\mathbf{b}_i - \mathbf{b}_j|} + q_i q_j \right. \\ & \times \left[6 \left(\frac{1}{|\mathbf{b}_i - \mathbf{b}_j|} - \frac{1}{L} \right) \theta(|\mathbf{b}_i - \mathbf{b}_j| - L) + 12 \right. \\ & \left. \left. \times \left(\frac{1}{|\mathbf{b}_i - \mathbf{b}_j|} - \frac{1}{\sqrt{2}L} \right) \theta(|\mathbf{b}_i - \mathbf{b}_j| - \sqrt{2}L) \right] \right\}. \quad (7) \end{aligned}$$

The first term in the sum is the standard Coulomb energy of the main cell, while the subsequent corrective terms are due to averaging over all lattice orientations. From Eq. (7) it is straightforward to extract the effective force between two charges at distance r , and we find that it has inoffensive *finite discontinuities* at $r = L$ and $r = \sqrt{2}L$. The θ functions activates only when one of the charges is sufficiently close to the box boundaries. Figure 2(b) illustrates the regions that are relevant for the corrections to the Coulomb potential. A necessary condition for the first corrective term [proportional to $\theta(r - L)$] to be nonzero is that a charge lies in the region outside a sphere of radius $L/2$ (the yellow sphere in Fig. 2 indicated with a thick arrow). Analogously a necessary condition for the second corrective factor [proportional to $\theta(r - \sqrt{2}L)$] to be nonzero is that a charge lies in the region near the corners of the main cell, at a distance larger than $L/\sqrt{2}$ from the center of the main cell (outside the blue regions indicated with a dashed arrow).

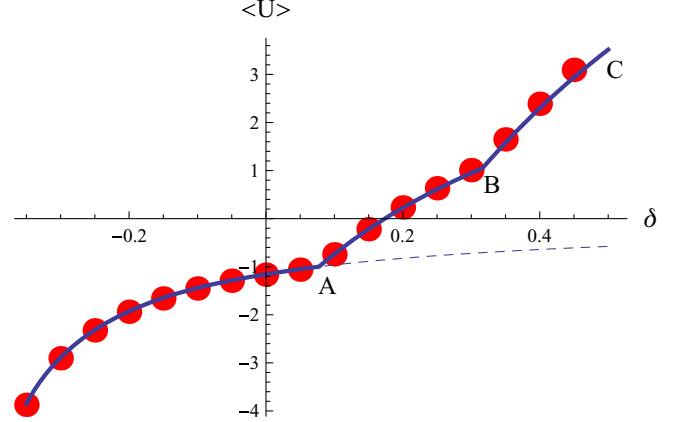


FIG. 3. (Color online) The red dots are numerical rotational averages of Ewald Eq. (2). The thick blue line is obtained by Eq. (7). The dashed curve is the energy of a pure Coulomb interaction (without any corrective term).

III. NUMERICAL TESTS

We promptly test our result with a simple example. Let us consider a cell of size $L = 1$ with $N = 2$ charges $q_1 = 1$ and $q_2 = -1$, at positions $\mathbf{b}_1 = \{-1/2, -1/2, -1/2\}$ and $\mathbf{b}_2 = \{\delta, \delta, \delta\}$, respectively. The parameter $\delta \in [-1/2, 1/2]$ can be used to test different regions inside the main cell. In particular, it enters the region where the first correction activates [yellow sphere in Fig. 2(b), i.e., $r = |\mathbf{b}_1 - \mathbf{b}_2| = 1$] at $\delta = (2\sqrt{3} - 3)/6 \approx 0.08$ and the region where the second corrections activates too [blue spherical domain in Fig. 2(b), i.e., $r = \sqrt{2}$] at $\delta = (2\sqrt{6} - 3)/6 \approx 0.32$.

In Fig. 3 the numerical rotational averages of the Ewald sum Eq. (2) at different values of δ are represented by red disks. They compare well with the plot of Eq. (7) (continuous thick curve). The plot is characterized by three regions: the first region where the two particles and the effective interaction is a pure Coulomb potential (up to point A), the second region where the two particles are at a distance such that the effective potential contains a contribution from the first θ function (from A to B), and the third region where both θ function corrections contributes to the total energy (from B to C). For comparison, we also plot the curve corresponding to a pure Coulomb interaction for all values of δ (dashed curve). From the plot it is evident that our method is different from the so-called *minimum image convention* [19]. In particular, the growth of the potential at large δ is quite a natural phenomenon in ionic systems where the dipolar term in the Ewald summation method is not neglected [20]. The deviations between our result and the numerical integration of the Ewald formula are simply due to numerical errors. While such errors can be reduced by increasing the numerical accuracy of the integration, they are, however, never completely avoidable since the infinite sums in the Ewald formula must be truncated somewhere necessarily, while our result Eq. (7) is finite and exact, and does not require any truncation.

In order to further illustrate the applicability of Eq. (7) in molecular simulations, we present here the result of a series of Monte Carlo (MC) simulations. We consider the NVT ensemble of a 1:1 restricted primitive model electrolyte for several

TABLE I. Average electrostatic energy per particle and heat capacity for a 1:1 electrolyte, at different molar concentrations.

ρ (M)	This work $\overline{U^*}/Nk_B T$	This work C_v/Nk_B	Ewald sums $\overline{U^*}/Nk_B T$	Ewald sums C_v/Nk_B
2	-0.6277 ± 0.0028	0.149 ± 0.020	-0.6556 ± 0.0045	0.139 ± 0.020
1	-0.5268 ± 0.0029	0.147 ± 0.020	-0.5493 ± 0.0030	0.141 ± 0.020
0.5	-0.4353 ± 0.0023	0.134 ± 0.018	-0.4544 ± 0.0022	0.138 ± 0.017
0.1	-0.2582 ± 0.0021	0.111 ± 0.015	-0.2703 ± 0.0029	0.104 ± 0.015
0.05	-0.1990 ± 0.0020	0.083 ± 0.011	-0.2089 ± 0.0019	0.087 ± 0.006
0.01	-0.1010 ± 0.0017	0.049 ± 0.007	-0.1067 ± 0.0016	0.051 ± 0.008
0.005	-0.0736 ± 0.0013	0.037 ± 0.005	-0.0785 ± 0.0006	0.039 ± 0.005
0.001	-0.0339 ± 0.0010	0.018 ± 0.003	-0.0372 ± 0.0010	0.017 ± 0.003
0.0005	-0.0244 ± 0.0007	0.012 ± 0.002	-0.0267 ± 0.0007	0.012 ± 0.002
0.0001	-0.0112 ± 0.0003	0.005 ± 0.001	-0.0127 ± 0.0006	0.005 ± 0.001
0.00005	-0.0079 ± 0.0004	0.004 ± 0.001	-0.0091 ± 0.0004	0.003 ± 0.001
0.00001	-0.0037 ± 0.0003	0.001 ± 0.001	-0.0044 ± 0.0002	0.001 ± 0.001

molar concentrations, (i) in the bulk, and (ii) around a charged macroparticle. All simulations were performed by using a standard Metropolis scheme [19,21], in a cubic simulation box of length L with periodic boundary conditions. Due to the spherical average, our system is not translational invariant and therefore in the calculation of the radial distribution functions (RDFs) we consider only particles that are inside a spherical shell S of radius $L/2$, centered in the cubic simulation box. Since any periodic charged particle which is located outside the spherical shell S is smeared on a homogeneous shell, it cannot be used in the calculation of the RDFs. Thus for the sake of simplicity we place one ion (or one macroparticle) at the center of the simulation box and use a cutoff $L/2$ to obtain the corresponding RDFs. The parameters for the 1:1 electrolyte simulations are the diameter of equal-sized ions $a = 4.25$ Å, the dielectric constant $\epsilon = 78.5$, the temperature $T = 298$ K, the valency $z_+ = |z_-| = 1$, and the total number of monovalent ions $N \approx 512$. The length L is fixed by the bulk electrolyte concentration. A Monte Carlo cycle consists of N attempts to move an arbitrary ion. The thermalization process takes about 5×10^4 MC cycles; all canonical averages are computed over a 2×10^5 MC sweep at full thermal equilibrium.

The electrostatic energy per particle, $\overline{U^*}/Nk_B T$, and the heat capacity C_v are defined via

$$U^* = \frac{\langle U \rangle}{4\pi\epsilon_0\epsilon}, \quad (8)$$

$$C_v = \frac{\overline{U^{*2}} - \overline{U^*}^2}{k_B T^2}, \quad (9)$$

where U^* corresponds to the total energy per cell in our approach, $\langle \dots \rangle$ is the canonical ensemble average, and k_B is the Boltzmann constant. Such quantities are shown in Table I for several electrolyte concentrations. For comparison, we list our results next to values obtained by the standard Ewald summation technique with conducting boundary conditions, and without taking spherical averages over all orientations of the infinite periodic lattice. From Table I, it is evident that the thermodynamic quantities calculated using our proposed

approach are of the same order of the standard Ewald summation method, which is a limit case in absence of angular rotations. Moreover, the RDFs in our approximation are similar to the ones obtained by the standard Ewald sum method, as one can see in Fig. 4 for a 2-M monovalent salt.

We consider also the case of an electrical double layer around a charged macroparticle. We use a macroparticle's diameter $D = 20$ Å at different valences $z_M = 4, 8, 12, 16, 20, 24, 28, 32$, for two electrolyte's concentrations: 0.01 and 2 M. An important quantity characteristic of this kind of Coulombic system is the mean electrostatic potential, which is defined by [22,23]

$$\psi(r) = \frac{e}{\epsilon_0\epsilon} \int_r^\infty \sum_{i=1}^2 z_i \rho_i g_i(t) \left[t - \frac{t^2}{r} \right] dt. \quad (10)$$

For both electrolyte concentrations, we calculated the mean electrostatic potential at the macroparticle's surface, ψ_0 , and at the Helmholtz plane, ψ_{HP} (which is defined as the closest approach distance between ions and the macroparticle).

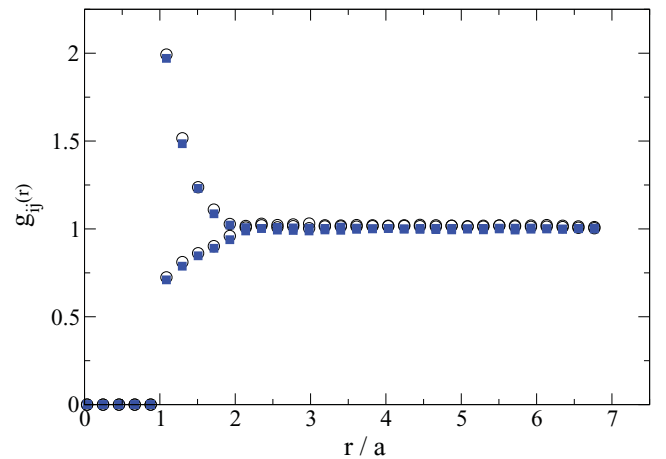


FIG. 4. (Color online) Radial distribution functions corresponding to a 1:1, 2-M bulk electrolyte in the restricted primitive model. Circles correspond to our approach and squares to Ewald sums.

TABLE II. Mean electrostatic potential at the surface (ψ_0) and at the Helmholtz plane (ψ_{HP}) around a charged macroparticle of valence z_M , in presence of a 1:1 electrolyte at a concentration 0.01 M.

z_M	This work	Ewald sums	This work	Ewald sums
	ψ_0 (mV) (± 2)	ψ_0 (mV) (± 2)	ψ_{HP} (mV) (± 2)	ψ_{HP} (mV) (± 2)
4	54.90	54.91	42.14	42.15
8	104.69	104.78	79.21	79.3
12	145.21	145.67	107.11	107.56
16	176.60	177.42	126.04	125.82
20	202.59	203.08	139.65	140.18
24	225.70	225.22	150.56	150.03
28	243.59	242.98	156.39	155.03
32	262.47	261.52	163.17	162.54

These results are summarized in Tables II and III, which exhibit similar values between the two approaches. The RDFs corresponding to a macroparticle of valence $z_M = 32$ are displayed in Fig. 5 for a 2-M monovalent salt, showing how the two different approximations have a similar behavior. In addition, the values of ψ_0 and ψ_{HP} as a function of the total number N of particles inside the simulation box for the same macroparticle are plotted in Fig. 6(a). Here, it is seen that our approach and the standard Ewald sums method display very similar values of the mean electrostatic potential and the same asymptotic behavior when the number of charged particles increases. Although the proposed method is $O(N^2)$ (as the standard Ewald summation method) its simplicity foresees a better performance in terms of computational speed. This is observed in Fig. 6(b), where the number of MC cycles per second performed as a function of the total number of charged particles are collated. For the number of particles reported, it is found that our approach can be from two to five times faster than the standard Ewald summation under analogous conditions.

TABLE III. Mean electrostatic potential at the surface (ψ_0) and at the Helmholtz plane (ψ_{HP}) around a charged macroparticle of valence z_M , in presence of a 1:1 electrolyte at a concentration 2 M.

z_M	This work	Ewald sums	This work	Ewald sums
	ψ_0 (mV) (± 1)	ψ_0 (mV) (± 1)	ψ_{HP} (mV) (± 1)	ψ_{HP} (mV) (± 1)
4	17.09	17.07	4.42	4.40
8	33.87	34.02	8.54	8.60
12	50.50	51.04	12.51	13.05
16	67.27	67.58	16.63	16.94
20	84.09	84.37	20.80	21.08
24	100.66	101.01	24.76	25.10
28	117.38	117.74	28.86	29.22
32	133.86	134.34	32.74	33.23

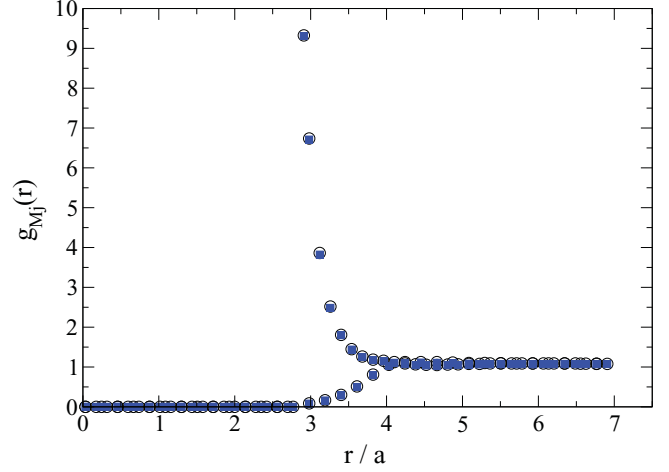


FIG. 5. (Color online) Radial distribution functions corresponding to a 1:1, 2-M electrolyte in the restricted primitive model around a charged macroparticle. The valence and diameter of the macroparticle are $D = 20 \text{ \AA}$ and $z_M = 32$, respectively. Circles correspond to our approach and squares to Ewald sums.

IV. CONCLUSIONS

The results in the last section show that the effective potential we present in this paper is suitable to application in simulations of ionic fluids. A major limitation of our result is that it is valid only for three-dimensional systems. One could easily derive an equivalent expression of Eq. (7) in two

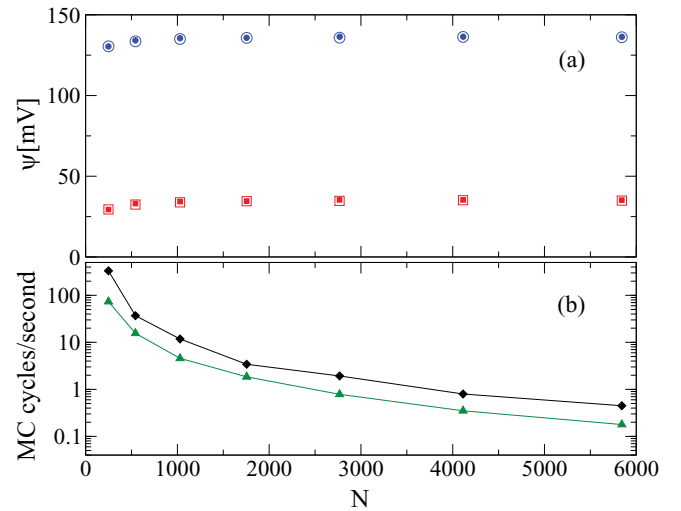


FIG. 6. (Color online) (a) Mean electrostatic potential at the macroparticle's surface (circles) and at the Helmholtz plane (squares) around a macroparticle as a function of the total number N of charged particles inside the simulation box. The macroparticle of valence and diameter $D = 20 \text{ \AA}$ and $z_M = 32$, respectively, is immersed in a 1:1, 2-M electrolyte in the restricted primitive model. The empty and filled symbols correspond to our proposed approach and Ewald summation method, respectively. (b) Number of Monte Carlo (MC) cycles per second as a function of the total number N of charged particles inside the simulation box. The diamonds and the triangles correspond to our proposed approach and Ewald summation method, respectively.

dimensions, but only for a logarithmic potential. In general, our arguments can be repeated for long-range potentials in d dimensions of the type $1/r^{d-2}$. We also emphasize that the dipolar term U_d in the Ewald summation formula Eq. (2) *must* be included and cannot be dropped in order to obtain a perfect match with Eq. (7). This is interesting because several works [19,21] discuss how the dipolar term can be dropped according to what kind of dielectric boundary conditions one imposes, while our formula has been derived without making any particular choice about the boundary conditions. Furthermore, we notice that in contrast with previous similar methods [14], ours does not rely on the homogeneity of the system *within* the main cell, which makes it suitable to study anisotropic systems frequently occurring in molecular biology and fluid state physics. As a final remark, Fig. 2(b) suggests that the effective energy in Eq. (7) is amenable to local computational algorithms, meaning that only the particles within the simulation box are sufficient for computing the total electrostatic energy of the rotational average of an infinite periodic lattice, despite the long-range nature of the interactions. Computational-intensive resources for evaluating special functions, or reciprocal lattices, are no longer necessary. Although our $O(N^2)$ method is outperformed by, for instance, a $O(N \log N)$ optimized Ewald summation scheme, its simplicity should be particularly appealing for implementations with parallel computing at an intermediate number of charges [17].

ACKNOWLEDGMENTS

G.V. and M.O.C. acknowledge the support of NSF Grant No. DMR-0907781, and G.I.G.-G. acknowledges the support of NSF Grant No. DMR-05020513.

APPENDIX: ELEMENTARY DERIVATION OF THE EWALD SUMMATION FORMULA

The energy per cell of a infinite periodic ionic lattice is defined as

$$U = \frac{1}{2} \sum_{\Lambda, i, j} ' \frac{q_i q_j}{D}, \quad D \equiv |\mathbf{b}_i - \mathbf{b}_j - \Lambda|. \quad (\text{A1})$$

It is convenient to introduce the following integral representation of the Coulomb potential:

$$\frac{1}{D} = \frac{2}{\sqrt{\pi}} \int_0^\infty dt e^{-D^2 t^2}. \quad (\text{A2})$$

The large- D behavior of Eq. (A2) is controlled by the integration over small- t values, and the small- D behavior is controlled by the integration over large- t values. Such an observation is relevant for the application of the Ewald method [2], which basically consists of decomposing the small-distance behavior of the integration domain from the large-distance behavior, and afterwards by tuning the movable boundary separating the two domains to achieve equal convergence rates for the two sums. Namely, by decomposing the integration region $\int_0^\infty = \int_0^\alpha + \int_\alpha^\infty$, and by using the integral

$$\int_\alpha^\infty dt e^{-D^2 t^2} = \frac{\sqrt{\pi}}{2D} \text{erfc}(\alpha D), \quad (\text{A3})$$

where $\text{erfc}(x)$ is the complementary error function:

$$\text{erfc}(x) = \frac{2}{\sqrt{\pi}} \int_x^\infty dt e^{-t^2}, \quad (\text{A4})$$

we obtain

$$U = \sum_{\Lambda, i, j} \frac{q_i q_j}{\sqrt{\pi}} \int_0^\alpha dt e^{-D^2 t^2} - \frac{\alpha}{\sqrt{\pi}} \sum_i q_i^2 + \sum_{\Lambda, i, j} \frac{q_i q_j}{2D} \text{erfc}(\alpha D). \quad (\text{A5})$$

In Eq. (A5) we added and subtracted the term with $D = 0$ in the first sum. That allows the application of the Poisson summation formula:

$$\sum_{\Lambda} f(\mathbf{x} + \Lambda) = \frac{1}{V} \sum_{\mathbf{Q}} e^{i\mathbf{x}\cdot\mathbf{Q}} \hat{f}(\mathbf{Q}), \quad (\text{A6})$$

where the reciprocal lattice is defined by $\mathbf{Q} \cdot \Lambda = 2\pi m$, $m \in \mathbb{Z}$, V is the volume of the primitive cell, and $\hat{f}(\mathbf{k})$ is the Fourier transform of $f(\mathbf{x})$:

$$\hat{f}(\mathbf{k}) \equiv \int_{\mathbb{R}^3} d^3\mathbf{x} e^{-i\mathbf{k}\cdot\mathbf{x}} f(\mathbf{x}). \quad (\text{A7})$$

We have

$$\begin{aligned} & \sum_{\Lambda, i, j} \frac{q_i q_j}{\sqrt{\pi}} \int_0^\alpha dt e^{-D^2 t^2} \\ &= \frac{1}{V \sqrt{\pi}} \sum_{\mathbf{Q}, i, j} q_i q_j e^{i(\mathbf{b}_i - \mathbf{b}_j) \cdot \mathbf{Q}} \int_{\mathbb{R}^3} d^3\mathbf{x} e^{-i\mathbf{Q}\cdot\mathbf{x}} \int_0^\alpha dt e^{-x^2 t^2} \\ &= \frac{\pi}{V} \sum_{\mathbf{Q}, i, j} q_i q_j e^{i(\mathbf{b}_i - \mathbf{b}_j) \cdot \mathbf{Q}} \int_0^\alpha dt \frac{1}{t^3} e^{-Q^2/4t^2} \\ &= \frac{2\pi}{V} \sum_{\mathbf{Q}} \hat{q}(\mathbf{Q}) \hat{q}(-\mathbf{Q}) \frac{e^{-Q^2/4\alpha^2}}{Q^2}, \end{aligned} \quad (\text{A8})$$

where

$$\hat{q}(\mathbf{Q}) \equiv \sum_j q_j e^{-i\mathbf{b}_j \cdot \mathbf{Q}}. \quad (\text{A9})$$

In the first line of Eq. (A8) we used the Poisson summation formula, then in the second line we evaluated the Gaussian integral over $d\mathbf{x}^3$, and finally we used the definition Eq. (A9). The final expression for U is

$$U = \frac{2\pi}{V} \sum_{\mathbf{Q}} \hat{q}(\mathbf{Q}) \hat{q}(-\mathbf{Q}) \frac{e^{-Q^2/4\alpha^2}}{Q^2} - \frac{\alpha}{\sqrt{\pi}} \sum_i q_i^2 + \sum_{\Lambda, i, j} \frac{q_i q_j}{2D} \text{erfc}(D\alpha). \quad (\text{A10})$$

The term $\mathbf{Q} = 0$ in the first sum requires special care. In fact, the asymptotic expansion at small Q of the argument in the sum is

$$\begin{aligned} \hat{q}(\mathbf{Q}) \hat{q}(-\mathbf{Q}) \frac{e^{-Q^2/4\alpha^2}}{Q^2} &\sim \frac{(\sum_i q_i)^2}{Q^2} \\ &+ \frac{\sum_{m,n} q_m q_n i(\mathbf{b}_m - \mathbf{b}_n) \cdot \mathbf{Q}}{Q} - \left[\frac{(\sum_i q_i)^2}{4\alpha^2} \right. \\ &\left. + \frac{1}{2} \sum_{m,n} q_m q_n \left((\mathbf{b}_m - \mathbf{b}_n) \cdot \frac{\mathbf{Q}}{Q} \right)^2 \right] + O(Q). \end{aligned} \quad (\text{A11})$$

The divergence of order $O(1/Q^2)$ is removed by the electroneutrality condition $\sum_i q_i = 0$, which also expunges the divergence of order $O(1/Q)$ and the first term of the $O(1)$ constant term. The remaining term is anisotropic. We therefore take its spherical average (for a more rigorous mathematical derivation of the same result, see [11])

$$\begin{aligned} & \frac{1}{4\pi} \int_0^\pi d\cos\theta \int_0^{2\pi} d\phi \frac{1}{2} \sum_{m,n} q_m q_n (\mathbf{b}_m - \mathbf{b}_n)^2 \cos^2\theta \\ &= \frac{1}{6} \sum_{m,n} q_m q_n (\mathbf{b}_m - \mathbf{b}_n)^2 = -\frac{1}{3} \sum_{m,n} q_m q_n \mathbf{b}_m \cdot \mathbf{b}_n \\ &= -\frac{1}{3} \left(\sum_m q_m \mathbf{b}_m \right)^2, \end{aligned} \quad (\text{A12})$$

which shows that the total dipole moment of the cell contributes to the Ewald sum. We can then write

Eq. (A10) as

$$\begin{aligned} U &= \frac{2\pi}{V} \sum_{\mathbf{Q} \neq 0} \hat{q}(\mathbf{Q}) \hat{q}(-\mathbf{Q}) \frac{e^{-Q^2/4\alpha^2}}{Q^2} - \frac{\alpha}{\sqrt{\pi}} \sum_i q_i^2 \\ &+ \sum_{\Lambda, i, j} \frac{q_i q_j}{2D} \operatorname{erfc}(D\alpha) + \frac{2\pi}{3V} \left(\sum_m q_m \mathbf{b}_m \right)^2, \end{aligned} \quad (\text{A13})$$

which is the final expression for the Ewald sum we used in this paper. Equation (A13) is independent from α . However, for numerical estimates the infinite sums must be truncated, and such a truncation yields a function $U(\alpha)$, which is α dependent. However, there is an interval of values for α where U is roughly constant. In our numerical utilizations of the Ewald method, we implemented the feature for α to be automatically selected in the region where $\partial U(\alpha)/\partial \alpha = 0$ [12]. Once α has been fixed, the Ewald method provides an efficient way to estimate the total electrostatic energy per cell of the periodic ionic lattice.

-
- [1] M. Karttunen, J. Rottler, I. Vattulainen, and C. Sagui, *Comp. Model. Membr. Bil.* **60**, 49 (2008).
- [2] P. P. Ewald, *Ann. Phys. (Leipzig)* **64**, 253 (1921).
- [3] C. Kittel, *Introduction to Solid State Physics*, 8th ed. (Wiley, New York, 2004).
- [4] E. Madelung, *Phys. Zs.* **19**, 524 (1918).
- [5] C. Sagui and T. A. Darden, *Annu. Rev. Biophys. Biomol. Struct.* **28**, 155 (1999).
- [6] U. Essmann, L. Perera, M. L. Berkowitz, T. Darden, H. Lee, and L. G. Pedersen, *J. Chem. Phys.* **103**, 8577 (1995).
- [7] C. Sagui and T. Darden, *J. Chem. Phys.* **114**, 6578 (2001).
- [8] A. C. Maggs and V. Rossetto, *Phys. Rev. Lett.* **88**, 196402 (2002).
- [9] M. M. Reif, V. Kräutler, M. A. Kastenzholz, X. Daura, and P. H. Hünenberger, *J. Phys. Chem. B* **113**, 3112 (2009).
- [10] E. V. Kholopov, *Phys. Usp.* **47**, 965 (2004).
- [11] S. W. de Leeuw, J. W. Perram, and E. R. Smith, *Proc. R. Soc. London, Ser. A* **373**, 27 (1980).
- [12] G. Hummer, *Chem. Phys. Lett.* **235**, 297 (1995).
- [13] D. J. Adams and G. S. Dubey, *J. Comput. Phys.* **72**, 156 (1987).
- [14] E. Yakub and C. Ronchi, *J. Chem. Phys.* **119**, 11556 (2003); *J. Low Temp. Phys.* **139**, 633 (2005); E. Yakub, *J. Phys. A* **39**, 4643 (2006).
- [15] X. Wu and B. R. Brooks, *J. Chem. Phys.* **122**, 044107 (2005); **129**, 154115 (2008).
- [16] E. Yakub, C. Ronchi, and D. Staicu, *J. Chem. Phys.* **127**, 094508 (2007); *J. Nucl. Mater.* **389**, 119 (2009).
- [17] P. K. Jha, R. Sknepnek, G. I. Guerrero-García, and M. Olvera de la Cruz, *J. Chem. Theor. Comput.* **6**, 3058 (2010).
- [18] D. Jackson, *Classical Electrodynamics*, 3rd ed. (John Wiley & Sons, New York, 1998).
- [19] M. P. Allen and D. J. Tildesley, *Computer Simulation of Liquids* (Clarendon, Oxford, 1989).
- [20] C. S. Hoskins and E. R. Smith, *Mol. Phys.* **41**, 243 (1980).
- [21] D. Frenkel and B. Smit, *Understanding Molecular Simulation* (Academic, San Diego, 2002).
- [22] E. González-Tovar and M. Lozada Cassou, *J. Phys. Chem.* **93**, 3761 (1989).
- [23] G. I. Guerrero-García, E. González-Tovar, M. Lozada Cassou, and F. de J. Guevara-Rodríguez, *J. Chem. Phys.* **123**, 034703 (2005).